Journal of Magnetic Resonance **152,** 109–123 (2001)
doi:10.1006/jmre.2001.2370, available online at http://www.idealibrary.com on IDEAL®

Carr–Purcell Sequences with Composite Pulses

M. D. Hürlimann

Schlumberger-Doll Research, Ridgefield, Connecticut 06877-4108

E-mail: hurlimann@ridgefield.sdr.slb.com

Received January 17, 2001; revised April 13, 2001; published online July 6, 2001

We present novel Carr–Purcell-like sequences using composite pulses that exhibit improved performance in strongly inhomogeneous fields. The sequences are designed to retain the intrinsic error correction of the standard Carr–Purcell–Meiboom–Gill (CPMG) sequence. This is achieved by matching the excitation pulse with the refocusing cycle such that the initial transverse magnetization lies along the axis $\hat{n}_{\mathcal{B}}$ characterizing the overall rotation of the refocusing cycle. Such sequences are suitable for relaxation measurements. It is shown that in sufficiently inhomogeneous fields, the echo amplitudes have an initial transient modulation that is limited to the first few echoes and then decay with the intrinsic relaxation time of the sample. We show different examples of such sequences that are constructed from simple composite pulses. Sequences of the form 90°_0–$(90^\circ_{90-\theta/2}$–$\theta_{180-\theta/2}$–$90^\circ_{90-\theta/2})^n$ with $\theta \approx 90^\circ$ and 270° generate signal over a bandwidth larger than that of the conventional CPMG sequence, resulting in an improved signal-to-noise ratio in inhomogeneous fields. The new sequence $127^\circ_{x,y}$–$(127^\circ_x$–$127^\circ_{-x})^n$ only excites signal off-resonance with a spectrum that is bimodal, peaking at $\Delta\omega_0 = \pm\omega_1$. Depending on the phase and exact timing of the first pulse, symmetric or antisymmetric excitation is obtained. We also demonstrate several new sequences with improved dependence on the RF field strength. The sequence $(22.5^\circ_{67.5}$–$90^\circ_{-22.5})$–$(90^\circ_{67.5}$–$45^\circ_{157.5}$–$90^\circ_{67.5})^n$ has the property that the phase of the signal depends on B_1, allowing coarse B_1 imaging in a one-dimensional experiment.

Key Words: **composite pulses; inhomogeneous fields; CPMG; relaxation.**

1. INTRODUCTION

The Carr–Purcell–Meiboom–Gill (CPMG) sequence (*1, 2*) is a standard sequence for measuring transverse relaxation times. It is well known that the Meiboom–Gill modification (*2*) compensates for the small inhomogeneities in the static field, B_0, and the RF field strength, B_1, that are unavoidable in any NMR apparatus. This makes it possible to refocus the transverse magnetization many times, limited only by the intrinsic relaxation time of the sample.

Over the past few years, several new NMR applications have been developed that operate in grossly inhomogeneous fields. These applications include strayfield NMR (*3*), well logging for oilfield applications (*4*), materials testing (*5*) and other applications with single-sided NMR systems. It has been recently shown that in these inhomogeneous fields, the CPMG sequence can still be used to measure the distribution of relaxation times (*6*).

The presence of large B_0 and B_1 field inhomogeneities complicates the spin dynamics considerably. The analysis of the CPMG sequence in inhomogeneous fields has been the subject of a series of recent papers (*6–11*). In (*6*) we showed that in sufficiently inhomogeneous fields, the amplitude of the first few echoes exhibits a transient behavior but quickly follows a smooth decay with a decay rate that is a weighted sum of $1/T_1$ and $1/T_2$. Therefore, it is still possible to measure relaxation time distributions in the presence of very large field inhomogeneities.

A practical application of this technique is the characterization of porous media filled with a wetting fluid. It has been shown that the distribution of T_2 relaxation times of the fluid is a measure of the distribution of pore sizes (*4*). In sedimentary rocks, these length scales can extend over more than three orders of magnitudes. To capture the complete relaxation decay, the CPMG sequence must be acquired with short enough echo spacing to measure the shortest decay time and with enough echoes to measure the longest decay time. In practice, this often requires the acquisition of several thousands echoes with submillisecond echo spacing.

When the inhomogeneity of the magnetic field, B_0, far exceeds the RF field strength, B_1, all pulses act as slice-selective pulses and only a small part of the sample contributes to the signal. In this paper, we address the question whether composite pulses can be used to increase the slice thickness, which improves the signal-to-noise ratio and efficiency of the RF power. Composite pulses have a rich history, but this is a new application and has not been investigated before. We first review briefly the relevant literature of previous work on composite pulses. In Section 2, we discuss our new strategy to design Carr–Purcell-like sequences with composite pulses. In Section 3, we illustrate this approach with a series of novel sequences using simple composite pulses that have different excitation bandwidths. We demonstrate experimentally that these sequences improve the signal-to-noise ratio and that they all can be used to measure relaxation times.

1090-7807/01 $35.00

In Section 4 we concentrate on modified sequences with novel dependencies on RF field strength, B_1.

Composite pulses were introduced in 1979 by Levitt and Freeman (*12*) to improve the performance of population inversion by the 180° pulse. Soon afterward, they demonstrated that composite pulses can also be used to improve the performance of the 180° pulse used as a refocusing pulse (*13*). They showed that in the presence of modest RF inhomogeneities, the 180°_y refocusing pulse should be replaced by the composite pulse 90°_x–180°_y–90°_x. When B_0 inhomogeneities are present, they suggested that 90°_x–270°_y–90°_x provides better compensation. Based on this pioneering work, longer composite pulses consisting of a concatenation of phase-shifted 90° pulses that improved the compensation for both B_0 and B_1 inhomogeneities simultaneously were developed (*14, 15*).

Tycko (*16*) introduced coherent averaging theory and the Magnus expansion to the analysis of composite pulses. This approach makes it possible to quantify the deviation of a given pulse from an ideal pulse in powers of $\Delta\omega_0$, $\Delta\omega_1$, or any other parameter of interest. Using this method, Tycko *et al.* (*17*) showed that the previously found composite pulse 90°_x–270°_y–90°_x compensates to first order for B_0 inhomogeneities and that the composite pulse 180°_0–180°_{120}–180°_0 compensates to first order for B_1 inhomogeneities. They also found longer sequences that compensate for B_0 or B_1 inhomogeneities to higher orders. Several different recursive expansion schemes (*18–21*) have been developed that allow the systematic construction of longer and longer composite pulses that compensate higher and higher orders of the Magnus expansion. A review of recursive expansions can be found in (*22*). Simbrunner and Stollberger (*8*) studied the error terms for the CPMG sequence with composite pulses proposed previously for modest inhomogeneities. They pointed out that these terms can be reduced by specific phase-shifting of the initial 90° pulse with respect to the refocusing pulses.

A different approach is based on the observation that in the Carr–Purcell sequence, two subsequent 180° pulses act ideally as a unity operator. However, B_1 and B_0 inhomogeneities will lead to deviations. By proper phase-shifting of subsequent 180° pulses, these deviations can be compensated to various degrees. Shaka *et al.* (*23*) demonstrated that by using the MLEV phase cycling schemes (*24*), the refocusing pulses treat *x* and *y* magnetization more symmetrically. Gullion *et al.* (*25, 26*) introduced a 16-step phase-cycling scheme they named XY-16. They showed that this approach is still effective in the presence of RF amplitude imbalance between the different channels.

Another interesting class of refocusing pulses is based on adiabatic fast passages (*27, 28*). Uğurbil *et al.* (*29, 30*) introduced equivalent 180° pulses that are composites of two half adiabatic fast passages and are effective even in very inhomogeneous B_1 fields. In 1991, Garwood and Ke (*31*) introduced a symmetric adiabatic pulse, named BIR-4, that improves the B_0 bandwidth while retaining the excellent B_1 performance. This pulse is a composite of one full and two half adiabatic fast passages with appropriate phase shifts between them. With such sequences, the B_0 bandwidth scales with the maximum strength of B_1, since the half adiabatic fast passage is only fully effective for B_0 offsets less than B_1. Pulses have been developed with even wider bandwidth by Conolly *et al.* (*32*) and by Hwang *et al.* (*33*). These pulses are composites of only full adiabatic fast passages. This way, the bandwidth is not limited by the strength of B_1, but only by the width and sweep rate of the frequency modulations.

Alternatively, when the 180° pulses in a CPMG sequence are replaced by single adiabatic fast passages, every even echo is refocused in inhomogeneous fields. Zweckstetter and Holak (*34*) have used this approach, complemented with MLEV phase cycling, to measure accurately the T_2 decay in modestly inhomogeneous fields over hundreds of echoes.

2. STRATEGY TO DESIGN COMPOSITE PULSES FOR GROSSLY INHOMOGENEOUS FIELDS

We are looking here for composite pulses for a new application: the pulses must be able to refocus the magnetization in grossly inhomogeneous fields repeatedly a large number of times, display an improved bandwidth, preserve the intrinsic error compensation scheme of the CPMG sequence, and not add any spurious time dependence on the decay of echo amplitudes that cannot be easily corrected.

To maximize the amplitude of a given echo in the presence of grossly inhomogeneous B_0 and B_1 fields, refocusing pulses containing elements of adiabatic fast passages, as discussed above, have the best performance. The main drawback of such pulses is that for a given maximum RF strength, B_1, these pulses are necessarily much longer than composite pulses based on hard RF pulses. The minimal echo spacing, t_E, is therefore much longer when adiabatic pulses are used. In our application, this could limit the detection of fast-decaying components. Even if the RF strength is high enough to allow short enough echo spacings, it is unlikely that these sequences will have overall higher signal-to-noise ratio. Short refocusing pulses can generate many more echoes in a given time, resulting in an overall higher signal-to-noise ratio. For our application, the same argument also favors simple composite pulses over the long, higher order composite pulses that were mentioned above. For this reason, we are concentrating here on short composite pulses. A generic form is shown in Fig. 1, where both the initial and refocusing pulses can consist of several phase-shifted RF pulses. We have also included a period τ_A of free precession following the initial composite pulse.

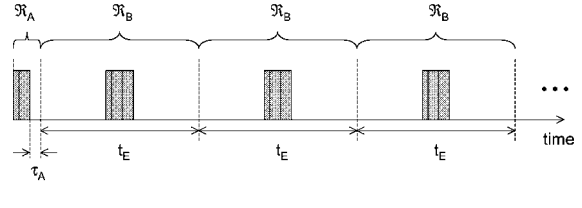

FIG. 1. Schematic pulse diagram of generic CPMG sequence with composite pulses.

2.1. Asymptotic Echo Amplitude

In the absence of relaxation or diffusion, the evolution for any composite pulse over a refocusing cycle can be described by a net rotation $\mathcal{R}_\mathcal{B}$, characterized by an axis $\hat{n}_\mathcal{B}$ and an angle $\alpha_\mathcal{B}$. Both the angle and the axis depend on the experimental parameters, the frequency offset, $\Delta\omega_0$, and the RF field strength, ω_1. Similarly, we can describe the evolution of the composite excitation pulse by a net rotation that we call $\mathcal{R}_\mathcal{A}$. Here we have ignored scalar couplings. Using this notation, the magnetization at the time of the formation of the Nth echo, $\mathbf{m}_N$, is given by (6, 9):

$$\mathbf{m}_N = \mathcal{R}_\mathcal{B}^N \, \mathcal{R}_\mathcal{A} \{\hat{z}\} = \mathcal{R}_\mathcal{B}(\hat{n}_\mathcal{B}, N\alpha_\mathcal{B}) \, \mathcal{R}_\mathcal{A} \{\hat{z}\}. \qquad [1]$$

Here we have assumed that the initial magnetization is along the $\hat{z}$ direction. The magnetization $\mathbf{m}_N$ is normalized with respect to its initial magnitude, M_0. In Eq. [1], the braces indicate the vector the rotations are operating on and the arguments in parentheses characterize the rotation by its axis and rotation angle.

As in (*23*), we could base the strategy for finding optimal composite pulses on identifying sequences that have a net resulting angle $\alpha_\mathcal{B}$ as close to π as possible over a wide range of frequency offsets and RF strengths. The evolution over two refocusing cycles approximates then the unity operator and in this ideal case, the initial magnetization $\mathcal{R}_\mathcal{A} \{\hat{z}\}$ is completely refocused at every second echo: $\mathbf{m}_{2k} = \mathcal{R}_\mathcal{A} \{\hat{z}\}$. However, Eq. [1] shows that any deviations of the angle from π accumulates from echo to echo. In order for this approach to work for thousands of echoes, as required in our application, the angle must be extremely close to π over the whole relevant range.

Our approach is based instead on the observation that for any rotation, one of the eigenvalues is always 1. The corresponding eigenvector is the axis of rotation, $\hat{n}_\mathcal{B}$. It is useful to rewrite Eq. [1] as

$$\begin{aligned}\mathbf{m}_N = {} & \hat{n}_\mathcal{B} \, (\hat{n}_\mathcal{B} \cdot \mathcal{R}_\mathcal{A} \{\hat{z}\}) \\ & + [\mathcal{R}_\mathcal{A} \{\hat{z}\} - \hat{n}_\mathcal{B}(\hat{n}_\mathcal{B} \cdot \mathcal{R}_\mathcal{A}\{\hat{z}\})] \cos(N\alpha_\mathcal{B}) \\ & + (\hat{n}_\mathcal{B} \times \mathcal{R}_A\{\hat{z}\}) \sin(N\alpha_\mathcal{B}). \end{aligned} \qquad [2]$$

The first term corresponds to the magnetization along the eigenvector with eigenvalue 1 and does not depend on the echo number N. In contrast, the second and third terms oscillate with a frequency $\alpha_\mathcal{B}$. The total signal is obtained by weighting the contributions of $\mathbf{m}_N(\Delta\omega_0, \omega_1)$ with the occurrences of $\Delta\omega_0$ and ω_1 in the sample. For large echo numbers, N, the second and third terms oscillate rapidly as a function of $\Delta\omega_0$ because the cosine and sine terms with the angle $N\alpha_\mathcal{B}$ enhance the modest frequency dependence of $\alpha_\mathcal{B}$. The frequency resolution of the acquired signal is limited by the acquisition time that is necessarily shorter than t_E. Therefore, in sufficiently inhomogeneous fields and high enough echo numbers N, the second and third terms will average out completely. After this initial transient period, only the first term in Eq. [2] contributes to the observed signal. The simple expression of the first term gives therefore the asymptotic echo

$$\mathbf{m}_\mathrm{asy} = \hat{n}_\mathcal{B} \, (\hat{n}_\mathcal{B} \cdot \mathcal{R}_\mathcal{A}\{\hat{z}\}). \qquad [3]$$

In strongly inhomogeneous fields, the asymptotic form [3] often applies already after the third echo, as shown below and in (*6*).

2.2. Optimization of Asymptotic Echo

The simple expression [3] for the asymptotic echo allows an efficient two-step strategy to optimize the ratio of signal-to-noise. Since only magnetization in the transverse plane can be detected, the effective axis of rotation, $\hat{n}_\mathcal{B}$, should lie completely in the transverse plane over as large a range of $\Delta\omega_0$ and ω_1 as possible. Given the refocusing pulse, the excitation pulse sequence $\mathcal{A}$ should then be chosen such that it rotates the vector $\hat{z}$ onto $\hat{n}_\mathcal{B}$ over the relevant range of inhomogeneities. Note that the optimization process naturally divides into two steps; the first one only involves the refocusing pulse, and the second step involves the excitation pulse:

- Refocusing pulse: maximize $\hat{n}_{\mathcal{B},\perp}$
- Excitation pulse: maximize $(\hat{n}_\mathcal{B} \cdot \mathcal{R}_\mathcal{A})$.

In most previous applications of composite pulses, it was important to generate pulses that had a certain overall rotation angle $\alpha_\mathcal{B}$. In contrast, in our application, $\alpha_\mathcal{B}$ is irrelevant. It is the direction of the axis $\hat{n}_\mathcal{B}$ that is crucial. For our application, it is more important that the 180°_y refocusing pulse is a "y pulse" than a "180° pulse."

It is not necessary that the direction of $\hat{n}_\mathcal{B}$ is constant within the transverse plane for all values of the offset frequency. If it is, the magnetization for all offset frequencies will be in phase at the end of the refocusing cycle and the spectrum of the echo is a pure absorption spectrum.

2.3. Effect of Relaxation on the Asymptotic Echo

The analysis above shows that in sufficiently inhomogeneous fields and in the absence of relaxation, the initial echo amplitudes show a transient behavior but then quickly approach a constant amplitude given by Eq. [3]. With relaxation, these later echo amplitudes will decay. In (*6*) we have analyzed the decay of the standard CPMG sequence with hard 180° pulses. The results also apply to a CPMG sequence with composite pulses: Relaxation leads to an exponential attenuation of the asymptotic echo amplitude with a decay rate that is a weighted average of $1/T_1$ and $1/T_2$:

$$\mathbf{m}_{\mathrm{asy},\perp}(kt_E) \simeq \hat{n}_{\mathcal{B},\perp} \, (\hat{n}_\mathcal{B} \cdot \mathcal{R}_\mathcal{A}\{\hat{z}\}) \, \exp\left\{-kt_E\left(\frac{n_{\mathcal{B},\perp}^2}{T_2} + \frac{n_{\mathcal{B},z}^2}{T_1}\right)\right\}. \qquad [4]$$

Equation [4] shows that when $T_1 \neq T_2$, the exact decay time depends on the offset frequency $\Delta\omega_0$ and RF strength, ω_1, through the dependence of $\hat{n}_{\mathcal{B}}$ and $\mathcal{R}_{\mathcal{A}}$ on these parameters. For large inhomogeneities, the initial decay rate is of the form

$$\frac{1}{T_{\text{eff}}} \simeq \frac{1}{T_2} - \frac{\langle n_{\mathcal{B},z}^2\, n_{\mathcal{B},\perp}(\hat{n}_{\mathcal{B}} \cdot \mathcal{R}_{\mathcal{A}}\{\hat{z}\})\rangle_{\Delta\omega_0,\omega_1}}{\langle n_{\mathcal{B},\perp}(\hat{n}_{\mathcal{B}} \cdot \mathcal{R}_{\mathcal{A}}\{\hat{z}\})\rangle_{\Delta\omega_0,\omega_1}} \left(\frac{1}{T_2} - \frac{1}{T_1}\right). \quad [5]$$

When $T_1 \neq T_2$, the decay is in general slower than T_2. The coefficient in front of the term $1/T_2 - 1/T_1$ is a positive constant <1 that must be determined for a given composite pulse, field inhomogeneity, and acquisition bandwidth. For large $\Delta\omega_0$ inhomogeneities, we find that the coefficient is typically in the range of 0.1 to 0.2.

2.4. Optimization of Sequence for Particular Field Inhomogeneity

For a field inhomogeneity that is characterized by a distribution function $f(\Delta\omega_0, \omega_1)$, the asymptotic echo shape without relaxation can be calculated from the transverse asymptotic magnetization, $m_{\text{asy},\perp}(\Delta\omega_0, \omega_1) \equiv m_{\text{asy},x} + i m_{\text{asy},y}$, given in Eq. [3] by Fourier transformation

$$m_{\text{asy}}(t) = \iint d\omega_1\, d\Delta\omega_0\; f(\Delta\omega_0, \omega_1) \times m_{\text{asy},\perp}(\Delta\omega_0, \omega_1) \exp\{i\Delta\omega_0 t\}, \quad [6]$$

where t is measured from the nominal echo center. To evaluate the spectrum $m_{\text{asy},\perp}(\Delta\omega_0, \omega_1)$, the effective axis $\hat{n}_{\mathcal{B}}$ of the refocusing cycle must be calculated as a function of $\Delta\omega_0$ and ω_1 for the particular composite pulse sequence. For this purpose, it is most convenient to take advantage of the expressions given by Counsell *et al.* (*35*): A rotation characterized by $(\hat{n}_1, \alpha_1)$ followed by a second rotation characterized by $(\hat{n}_2, \alpha_2)$, is described by a net rotation around an axis $\hat{n}_{12}$ and an angle α_{12} given by

$$\cos\left(\frac{\alpha_{12}}{2}\right) = \cos\left(\frac{\alpha_1}{2}\right)\cos\left(\frac{\alpha_2}{2}\right) - \sin\left(\frac{\alpha_1}{2}\right)\sin\left(\frac{\alpha_2}{2}\right)\hat{n}_1 \cdot \hat{n}_2 \quad [7]$$

$$\sin\left(\frac{\alpha_{12}}{2}\right)\hat{n}_{12} = \sin\left(\frac{\alpha_1}{2}\right)\cos\left(\frac{\alpha_2}{2}\right)\hat{n}_1 + \cos\left(\frac{\alpha_1}{2}\right)\sin\left(\frac{\alpha_2}{2}\right)\hat{n}_2 - \sin\left(\frac{\alpha_1}{2}\right)\sin\left(\frac{\alpha_2}{2}\right)\hat{n}_1 \times \hat{n}_2. \quad [8]$$

For optimal detection, a window function matched to this echo shape should be used. The resulting signal power-to-noise ratio is proportional to

$$\frac{S}{N} \propto \int_{-T/2}^{T/2} dt\, m_{\text{asy}}(t)\, m_{\text{asy}}^*(t), \quad [9]$$

where T is the duration of the acquisition window and is necessarily shorter than t_{E}.

This formulation of the problem lends itself to an optimization using a computer search routine that maximizes the signal-to-noise ratio, Eq. [9], for the particular inhomogeneity, $f(\Delta\omega_0, \omega_1)$. It is straightforward to add extra experimental constrains to the optimization problem, such as maximum peak power, overall duration of composite pulse, or minimum step size for phase and amplitude. For different optimization functions, such an approach has been demonstrated previously for instance by Lurie (*36*), Poon and Henkelman (*37, 38*), and Bai *et al.* (*39*).

3. EXAMPLES OF SPECIFIC COMPOSITE PULSES

In the rest of this paper, rather than presenting results of composite pulse obtained by computer optimization for a specific field inhomogeneity and experimental constraints, we investigate the properties of some new, but simple composite pulses. These individual composite pulses can then be used as building blocks for the construction of overall sequences that still have the inherent error correction of the standard CPMG sequence, but different responses with respect to frequency offsets or RF field strength. Such sequences can also be used as starting points in computer searches for more refined sequences, reducing the phase space that must be searched in the optimization process.

We will start with the standard CPMG sequence with hard 90° and 180° pulses, discuss different phase cycling schemes, and explain the role of the delay $\tau_{\mathcal{A}}$ indicated in Fig. 1. Then we discuss refocusing pulses of the form 90°–θ–90°. CPMG sequences using such pulses have been discussed before for small field inhomogeneities (*8*). Here we study the performance for general inhomogeneities and discuss the optimal value of $\tau_{\mathcal{A}}$. We then discuss a new type of refocusing pulse suitable only for inhomogeneous fields. This novel pulse refocuses perfectly at offset frequencies $\Delta\omega_0 = \pm\omega_1$, but not on resonance, $\Delta\omega_0 = 0$. In Section 4, we focus on composite pulses that display novel dependencies on RF field strengths.

To test the theoretical analysis, we have performed proton NMR experiments in the fringefield of a Nalorac 2-T superconducting magnet on a sample of water that is slightly doped with NiCl to reduce the relaxation time to around 100 ms. The sample was placed on-axis 50 cm outside the magnet, where the field strength is 41.4 mT with a gradient of 132 mT/m. A Teflon rod was placed vertically in the RF coil that is tuned to the Larmor frequency of 1.765 MHz. Within this Teflon rod, the sample cell is a 2-cm long cylindrical cell of 2 cm diameter, oriented horizontally along the gradient direction. An Apollo Tecmag spectrometer was used for the pulse generation and signal acquisition. The nominal RF pulse amplitude was $\omega_{1,0} = 2\pi \times 10$ kHz with a resulting pulse duration of $t_{90} = 25\mu$s.

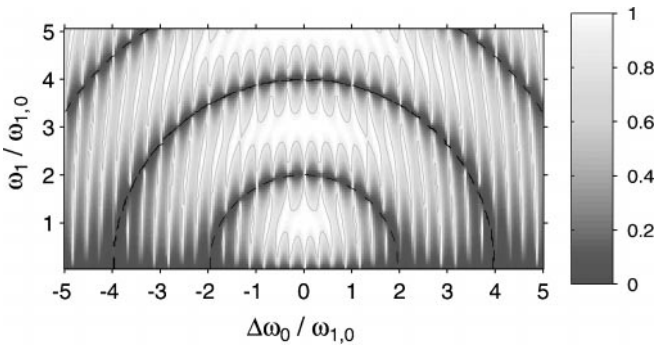

FIG. 2. Transverse component $n_{\mathcal{B},y}$ of the axis describing the refocusing cycle for a standard 180°_y pulse as a function of normalized frequency offset, $\Delta\omega_0/\omega_{1,0}$, and RF field strength, $\omega_1/\omega_{1,0}$. Here $\omega_{1,0} = \gamma B_{1,0}$ is the nominal RF field strength with $\omega_{1,0}t_{180} = \pi$. The echo spacing was assumed to be $t_E = 7t_{180}$. The solid contour lines indicate $n_{\mathcal{B},y} = 0.9$, the dashed ones indicate $n_{\mathcal{B},y} = 0$.

3.1. *Standard CPMG Sequence with* 180° *Refocusing Pulses*

The direction of the net axis $\hat{n}_\mathcal{B}$ as a function of offset frequency and RF field strength for a refocusing cycle consisting of a hard 180°_y pulse between two periods of free precession can be obtained by repeatedly applying the expressions [7] and [8] and is plotted in Fig. 2. Explicit expressions can be found in (*6*). For symmetry reasons, the transverse component, $\hat{n}_{\mathcal{B},\perp}$, always lies along the $\hat{y}$ axis. Therefore, the asymptotic magnetization $\mathbf{m}_{\text{asy}}$ has only components in the $\hat{y}$ channel. With a hard 180° refocusing pulse, Eq. [3] shows that the largest possible asymptotic transverse magnetization is $n_{\mathcal{B},y}$. This is achieved if the initial pulse tips the magnetization exactly along $\hat{n}_\mathcal{B}$.

3.1.1. Phasing. With a simple hard 90° pulse as initial excitation pulse, Eq. [3] shows that the phase of the initial 90° pulse should be phase-shifted relative to the refocusing pulses by 90° to maximize the projection of the resulting magnetization, $\mathcal{R}_\mathcal{A}\{\hat{z}\}$, onto the axis $\hat{n}_\mathcal{B}$. This is exactly the Meiboom and Gill modification (*2*). In practice, this phase shift is alternated between $+90^\circ$ and -90° in successive acquisitions and the measured signal is added and subtracted. This basic phase cycling scheme eliminates any dc offsets and any signal that was not generated by the initial 90° pulse. In our spin dynamics calculation, this phase cycling is included by eliminating the z component of $\mathcal{R}_\mathcal{A}\{\hat{z}\}$. As a consequence, the largest possible asymptotic transverse magnetization is reduced to $n^2_{\mathcal{B},y}$ from $n_{\mathcal{B},y}$ mentioned above.

Bãlibanu *et al.* (*10*) found numerically that the modified sequence 90°_x–$(180^\circ_x$–$180^\circ_{-x})^n$ gives essentially identical results to the standard CPMG sequence, 90°_x–$(180^\circ_y)^n$. This can be understood most easily as follows: The standard CPMG sequence in the rotating frame rotating at the RF frequency, ω_{RF}, appears as the modified sequence in a rotating frame that rotates at a slightly different frequency, $\omega_{\text{RF}} \pm \pi/t_E$. This equivalence holds as long as the pulse duration is much shorter than the echo spacing. Therefore, the modified sequence corresponds to the standard CPMG sequence with a small frequency offset of π/t_E. In inhomogeneous fields where this frequency offset is negligible, the two sequences give therefore the same response.

3.1.2. Optimization of $\tau_\mathcal{A}$. The magnetization following a standard 90°_x pulse of duration t_{90} is given by

$$u_x = -\frac{\Delta\omega_0\omega_1}{\Omega^2}(1 - \cos\Omega t_{90})$$
$$u_y = \frac{\omega_1}{\Omega}\sin\Omega t_{90}, \qquad [10]$$

where $\Omega = \sqrt{\Delta\omega_0^2 + \omega_1^2}$ is the nutation frequency. In Fig. 3 the in-phase component, u_y, and out-of-phase component, $-u_x$, are plotted as a function of offset frequency and RF field strength. The expression for the asymptotic echo, Eq. [3], shows that only the component of the initial magnetization along the net axis, $\hat{n}_\mathcal{B}$, is refocused. Since for the standard 180°_y refocusing pulse, $\hat{n}_\mathcal{B}$ has only components in the $\hat{y}$–$\hat{z}$ plane, the out-of-phase component $-u_x$ does not contribute to the asymptotic echo.

The overall phase shift between the initial excitation pulse and the refocusing pulses in the Meiboom and Gill modification was chosen to maximize the projection of the initial transverse magnetization onto $\hat{n}_\mathcal{B}$ close to resonance. The frequency range over which the projection is optimized can be significantly increased

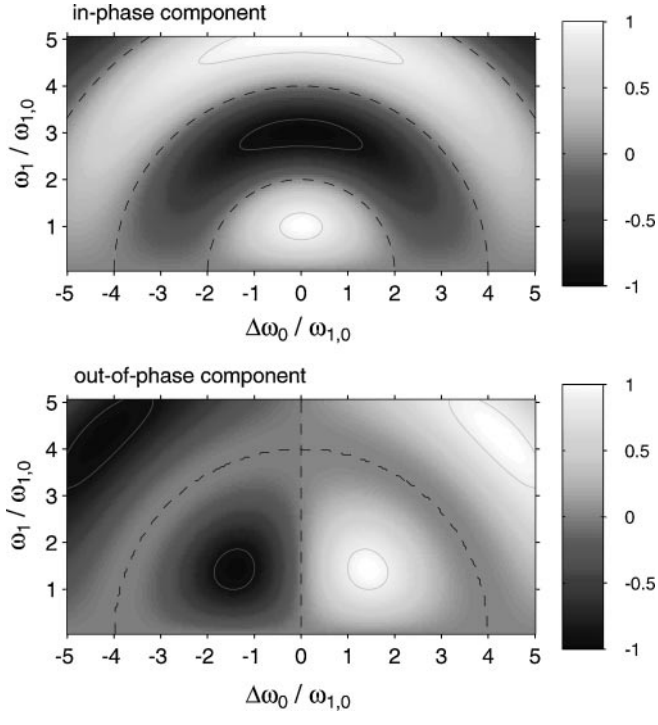

FIG. 3. Transverse magnetization, $m_{x,y}$, following a single 90°_x pulse as a function of normalized frequency offset, $\Delta\omega_0/\omega_{1,0}$, and RF field strength, $\omega_1/\omega_{1,0}$. Top panel shows in-phase component, m_y, and bottom panel shows out-of-phase component, m_x. The magnetization is normalized with respect to M_0. The solid contour lines indicate $m_{x,y} = \pm 0.9$, the dashed ones indicate $m_{x,y} = 0$.

by adjusting the time $\tau_{\mathcal{A}}$ shown in Fig. 1. Close to resonance, $\Delta\omega_0 \approx 0$, the deviation of the phase of the initial transverse magnetization, $\phi_{\mathcal{A}} = -\arctan(u_x/u_y)$ is linear in offset frequency, $\Delta\omega_0$. Analogous to the standard process of phasing of NMR spectra, we compensate this linear phase deviation by including a period $\tau_{\mathcal{A}}$ of free precession. We have previously shown (*40*) that for the standard CPMG sequence, the optimal value for $\tau_{\mathcal{A}}$ is given by

$$\tau_{\mathcal{A}} = \frac{\cos(\omega_1 t_{90}) - 1}{\omega_1 \sin(\omega_1 t_{90})}. \qquad [11]$$

For RF field strengths close to the nominal value, $\omega_{1,0}$, this time interval is given by

$$\tau_{\mathcal{A}} = -2t_{90}/\pi. \qquad [12]$$

The negative sign indicates that the initial pulse interval should be *reduced* by $2t_{90}/\pi$. This result can be interpreted as follows: The magnetization following the real 90° pulse can be thought of as being generated by a fictitious pulse a time $|\tau_{\mathcal{A}}|$ earlier. The in-phase magnetization of this fictitious pulse is given by $u_{y,\mathrm{opt}} = u_y \cos(\Delta\omega_0\tau_{\mathcal{A}}) + u_x \sin(\Delta\omega_0\tau_{\mathcal{A}})$ and is plotted in Fig. 4. The refocusing cycles, characterized by $\mathcal{R}_{\mathcal{B}}$, operate on this fictitious magnetization that appears a time t_{E} before the first echo. From a comparison of Fig. 3 and Fig. 4, it is apparent that by choosing the correct value of $\tau_{\mathcal{A}}$, the bandwidth of the initial transverse magnetization with the correct phase can be significantly increased.

Experimental verification is shown in Fig. 5. The top two panels compare the first 10 echoes measured with the standard CPMG sequence using $\tau_{\mathcal{A}} = 0$ (A) and $\tau_{\mathcal{A}} = -2t_{90}/\pi$ (B). After the first echo, the adjusted sequence generates echoes larger than those of the standard sequence. The data also show that the limiting shape of the echoes depends on the initial timing of the sequence. This demonstrates that the timing affects the signal bandwidth. It is also apparent that with the improved timing, the shapes of the echoes approach the asymptotic shape faster than with the standard timing. With the adjusted timing, the second and third terms in Eq. [2], which give rise to the transient effect in the initial echo amplitude, are minimized.

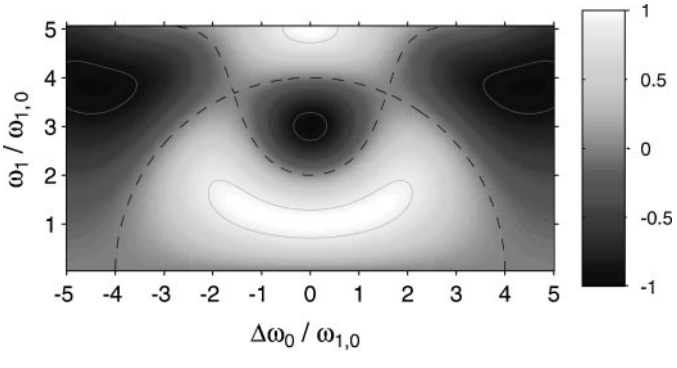

FIG. 4. In-phase magnetization, m_y, following a 90°_x pulse and a period of free precession, $\tau_{\mathcal{A}} = -2t_{90}/\pi$. The magnetization is normalized with respect to M_0, the solid contour lines indicate $m_y = \pm 0.9$, and the dashed ones indicate $m_y = 0$. The magnetization immediately after a 90° pulse, shown in Fig. 3, can be thought of as being generated by a fictitious pulse at time $2t_{90}/\pi$ earlier with the in-phase response shown here. This fictitious pulse has a much broader bandwidth for in-phase magnetization when $\omega_1 \simeq \omega_{1,0}$.

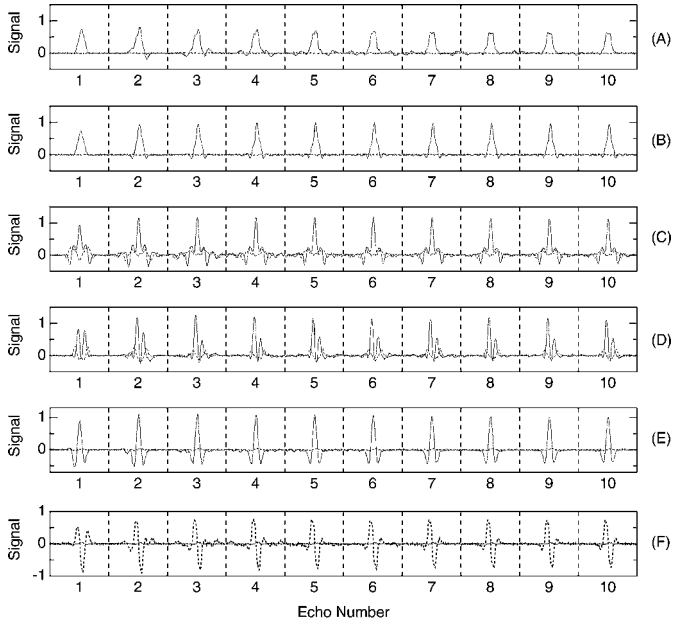

FIG. 5. Experimental results of the initial 10 echoes measured with different CPMG-like pulse sequences in a constant gradient. For each echo, the acquisition window is 256 μs long with an echo spacing of 1 ms. The RF field strength was set to $\omega_1 = 2\pi \times 10$ kHz. In-phase signal is shown as a solid line, out-of-phase signal is dashed. (A) Standard CPMG sequence 90°_0–$(180^\circ_{90})^n$ with $\tau_{\mathcal{A}} = 0$. (B) Same as A, except $\tau_{\mathcal{A}} = -2t_{90}/\pi$. (C) CPMG with Levitt-type composite pulse with $\theta = 270^\circ : 90^\circ_0$–$(90^\circ_{135}$–$270^\circ_{225}$– $90^\circ_{135})^n$ with $\tau_{\mathcal{A}} = -2t_{90}/\pi$. (D) CPMG with Levitt-type composite pulse with $\theta = 90^\circ : 90^\circ_0$–$(90^\circ_{45}$–$90^\circ_{135}$–$90^\circ_{45})^n$ with $\tau_{\mathcal{A}} = 0$. (E) Symmetric off-resonance sequence 127°_0–$(127^\circ_0$–$127^\circ_{180})^n$ with $\tau_{\mathcal{A}} = -t_{90}$. (F) Antisymmetric off-resonance sequence 127°_{90}–$(127^\circ_0$–$127^\circ_{180})^n$ with $\tau_{\mathcal{A}} = 0$.

For different refocusing pulses discussed below, the axis $\hat{n}_{\mathcal{B}}$ is not always confined to the $\hat{y}$–$\hat{z}$ plane. In such cases, the same approach can still be used to compensate the dispersion of the directions to first order, but the optimal value for $\tau_{\mathcal{A}}$ will be in general different from Eq. [11]. Similarly, different excitation pulses will result in different optimal values for $\tau_{\mathcal{A}}$. As an example, the half adiabatic fast passage is an excitation pulse sequence that can be used to generate transverse magnetization that is all in the $\hat{y}$ channel. In the limit of a slow frequency sweep, the resulting transverse magnetization is $u_x = 0, u_y = \omega_1/\Omega$. In this case, the direction of the transverse magnetization and that of the transverse component of the axis $\hat{n}_{\mathcal{B}}$ are identical and the optimal value is $\tau_{\mathcal{A}} = 0$. It is interesting to note that despite this property, at the nominal value of RF field strength $\omega_1 = \omega_{1,0}$, the excitation bandwidth of the CPMG sequence

using the half adiabatic fast passage is smaller than the bandwidth for the standard CPMG with a hard 90°_x pulse and the optimal value of $\tau_{\mathcal{A}}$.

3.2. *Levitt-Type Composite Refocusing Pulse*

The first 180° composite pulses introduced by Levitt and Freeman (*12*) were of the form 90°_x–θ_y–90°_x. Using Eqs. [7] and [8] it is easy to show that on resonance and at the nominal RF field strength, the net axis $\hat{n}_{\mathcal{B}}$ for such composite pulses is always in the transverse plane, but not pointing along the $\hat{x}$ direction: $\hat{n}_{\mathcal{B}} = \cos(\theta/2)\hat{x} + \sin(\theta/2)\hat{y}$. In order to use such composite pulses as refocusing pulses in place of a 180°_y pulse, the composite pulse must be phase-shifted relative to the initial 90° pulse by 90°–$\theta/2$. This corresponds to the generalized Meiboom–Gill modification. With these phase-shifted composite pulses, we can construct a whole family of new pulse sequences that are of the form

$$90^\circ_0\text{–}\left(90^\circ_{90-\theta/2}\text{–}\theta_{180-\theta/2}\text{–}90^\circ_{90-\theta/2}\right)^n. \qquad [13]$$

Like the standard CPMG sequence, these sequences compensate for small pulse imperfections and result in a large asymptotic echo, because the initial magnetization is predominantly collinear with the net axis $\hat{n}_{\mathcal{B}}$. The direction of $\hat{n}_{\mathcal{B}}$ for these composite pulses is not confined anymore to the $\hat{y}$–$\hat{z}$ plane as was the case for the standard CPMG sequence. As a consequence, the asymptotic echo can have both in- and out-of-phase components, and the optimum value of $\tau_{\mathcal{A}}$ will be in general different from the previous value of $-2t_{90}/\pi$. In order to choose the optimal value of θ for a specific problem, we must study the dependence of $\hat{n}_{\mathcal{B}}$ over the relevant values of offset frequency, $\Delta\omega_0$, and RF field strength, ω_1. Within this family of composite pulses, the optimization procedure reduces to a two-dimensional search in the θ–$\tau_{\mathcal{A}}$ plane.

One example of such a sequence with $\theta = 270^\circ$ has been previously studied by Simbrunner and Stollberger (*8*) for moderately inhomogeneous fields. The composite 180° pulse 90°_y–270°_x–90°_y was initially found by Levitt and Freeman (*13*) to compensate for modest $\Delta\omega_0$ inhomogeneities and Tycko (*16*) showed that this pulse sequence compensates for $\Delta\omega_0$ inhomogeneities in the lowest order of the Magnus expansion. In Fig. 6, the transverse components of $\hat{n}_{\mathcal{B}}$ of a refocusing cycle with a 90°_{135}–270°_{225}–90°_{135} composite pulse are shown. Compared to the standard refocusing pulse shown in Fig. 2, the sweet spots of $\hat{n}_{\mathcal{B}}$ near the values of $(\Delta\omega_0 = 0, \omega_1/\omega_{1,0} = 2n-1)$ are broader with respect to $\Delta\omega_0$, but narrower with respect to ω_1. Figure 5C shows the first 10 echoes measured with these refocusing pulses in a constant gradient and the nominal RF field strength, $\omega_{1,0}$. The echo peak is indeed higher than with the previous sequences. It is also apparent that in this case, echo signal appears in both channels and cannot be phased into a single channel, even though the range of Larmor frequencies in this sample is symmetric.

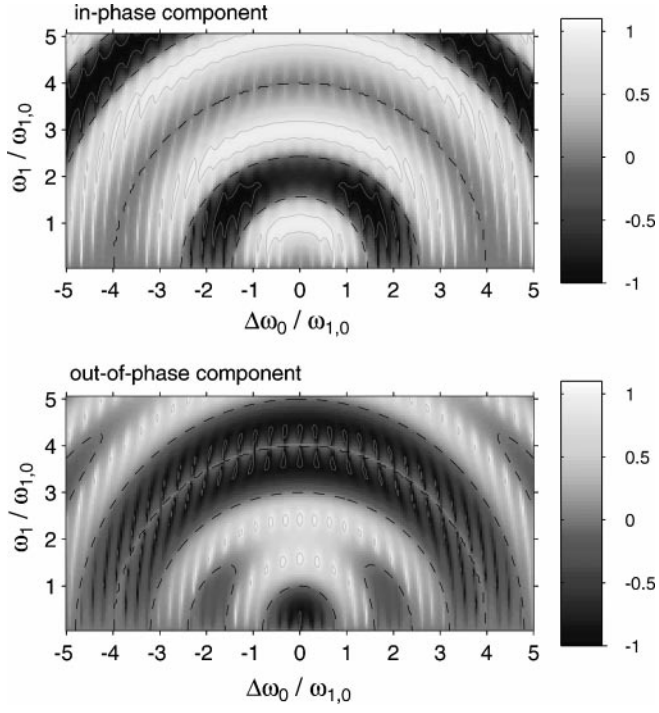

FIG. 6. Transverse components of axis characterizing refocusing cycle with composite pulse 90°_{135}–270°_{225}–90°_{135} as a function of normalized frequency offset, $\Delta\omega_0/\omega_{1,0}$, and RF field strength, $\omega_1/\omega_{1,0}$. Top panel shows the in-phase component, $n_{\mathcal{B},y}$ and the bottom panel the out-of-phase component, $-n_{\mathcal{B},x}$. The echo spacing was assumed to be $t_{\mathrm{E}} = 7t_{180}$. The solid contour lines indicate $n_{\mathcal{B},i} = \pm 0.9$, the dashed lines indicate $n_{\mathcal{B},i} = 0$. The in-phase component has a wider sweet spot near $\omega_1 \simeq \omega_{1,0}$ for this composite pulse than for the standard 180° pulse, shown in Fig. 2.

In Fig. 7, we show the transverse components of $\hat{n}_{\mathcal{B}}$ for another Levitt-type refocusing pulse with $\theta = 90^\circ$. In this case, the sweet spot at $(\Delta\omega_0/\omega_{1,0}, \omega_1/\omega_{1,0}) = (0, 1)$ is reduced compared to the previous sequences. However as compensation, this composite pulse is able to refocus magnetization far off-resonance in a region around $(\Delta\omega_0/\omega_{1,0}, \omega_1/\omega_{1,0}) = (\pm\sqrt{2}, \sqrt{2})$. On resonance, it refocuses the initial y magnetization. Off resonance, it is the initial x magnetization that gets refocused. To take advantage of this property, the initial excitation pulse must be chosen such as to maximize $(\hat{n}_{\mathcal{B}} \cdot \mathcal{R}_{\mathcal{A}}\{\hat{z}\})$ over the whole range. Figure 3 shows that the simple 90°_x pulse is well suited for this purpose. In this case, it is necessary to choose $\tau_{\mathcal{A}} = 0$. Note that the asymptotic magnetizations, calculated with Eq. [3] for the nominal echo center, have opposite sign for $\Delta\omega_0 = \pm\sqrt{2}\omega_{1,0}$ and appear in the out-of-phase channel. Therefore, these contributions interfere destructively at the nominal echo center, but interfere constructively at a time $\pm t_{90}/\sqrt{2}$ from the nominal echo center and give rise to an antisymmetric signal in the in-phase channel. This is superimposed to the symmetric signal from the contribution close to resonance. In Fig. 5D, it is demonstrated experimentally that the combined effect results in echo amplitudes larger than those obtained with the standard CPMG sequence. This advantage only exists in sufficiently inhomogeneous fields.

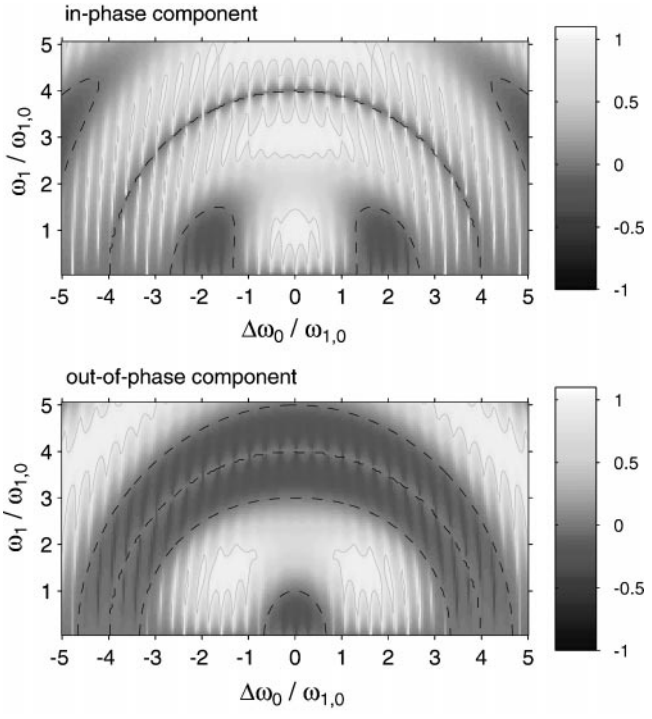

FIG. 7. Transverse components of axis characterizing refocusing cycle with composite pulse 90°_{45}–90°_{135}–90°_{45} as a function of normalized frequency offset, $\Delta\omega_0/\omega_{1,0}$, and RF field strength, $\omega_1/\omega_{1,0}$. Top panel shows the in-phase component, $n_{\mathcal{B},y}$ and the bottom panel the out-of-phase component, $-n_{\mathcal{B},x}$. The echo spacing was assumed to be $t_E = 7t_{180}$. The solid contour lines indicate $n_{\mathcal{B},i} = \pm 0.9$, the dashed lines indicate $n_{\mathcal{B},i} = 0$.

3.3. *Off-Resonance Pulses*

We give here even clearer examples of pulse sequences that can be used to refocus magnetization repeatedly in inhomogeneous fields, but that are completely ineffective in homogeneous fields. These sequences are based on the new composite refocusing pulse 127°_x–127°_{-x}. The pulse angles are chosen to be $\sqrt{2}\cdot 90^\circ = 127.3^\circ$. On resonance, the two 127° pulses offset each other and have no net effect on the spin dynamics. However, off resonance at $(\Delta\omega_0/\omega_{1,0}, \omega_1/\omega_{1,0}) = (\pm 1, 1)$, the two pulses rotate the magnetization around two perpendicular axes with a nutation angle Ωt_{127} of 180°. This is illustrated in Fig. 8, where we display the y component of the net axis $\hat{n}_{\mathcal{B}}$ for the complete refocusing cycle consisting of the period of free precession, the composite pulse 127°_x–127°_{-x}, and another period of free precession. Note that with this composite pulse, the net rotation axis $\hat{n}_{\mathcal{B}}$ always lies in the $\hat{y}$–$\hat{z}$ plane, independent of offset frequency or RF field strength. This composite 180° pulse can refocus magnetization near $(\Delta\omega_0/\omega_{1,0}, \omega_1/\omega_{1,0}) = (\pm[2k-1], [2k-1])$, where k is an integer. This should be compared to the standard 180°_y pulse that refocuses magnetization near $(\Delta\omega_0/\omega_{1,0}, \omega_1/\omega_{1,0}) = (0, [2k-1])$.

There are two simple ways to excite initial transverse magnetization collinear with $\hat{n}_{\mathcal{B}}$ of this composite pulse. Both methods

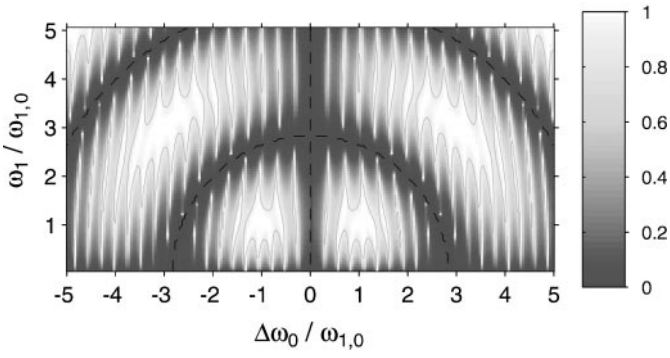

FIG. 8. In-phase component, $n_{\mathcal{B},y}$, of axis-characterizing refocusing cycle with composite pulse $\sqrt{2}90^\circ_0$–$\sqrt{2}90^\circ_{180}$ as a function of normalized frequency offset, $\Delta\omega_0/\omega_{1,0}$, and RF field strength, $\omega_1/\omega_{1,0}$. The out-of-phase component $n_{\mathcal{B},x}$ vanishes for all offset frequencies and RF field strengths. The echo spacing was assumed to be $t_E = 7t_{180}$. The solid contour lines indicate $n_{\mathcal{B},y} = 0.9$, the dashed lines indicate $n_{\mathcal{B},y} = 0$. The sweet spots are at $\Delta\omega_0/\omega_{1,0} = \pm(2k-1)$; $\omega_1/\omega_{1,0} = 2k-1$, with $k = 1, 2, \ldots$.

are based on a single 127° excitation pulse and are illustrated in Fig. 9. At an off-resonance frequency of $\Delta\omega_0 = \pm\omega_{1,0}$ and the nominal RF field strength $\omega_{1,0}$, a 127°_y pulse rotates the initial $\hat{z}$ magnetization onto the $\pm\hat{y}$ axis. In this case, $\tau_{\mathcal{A}} = 0$

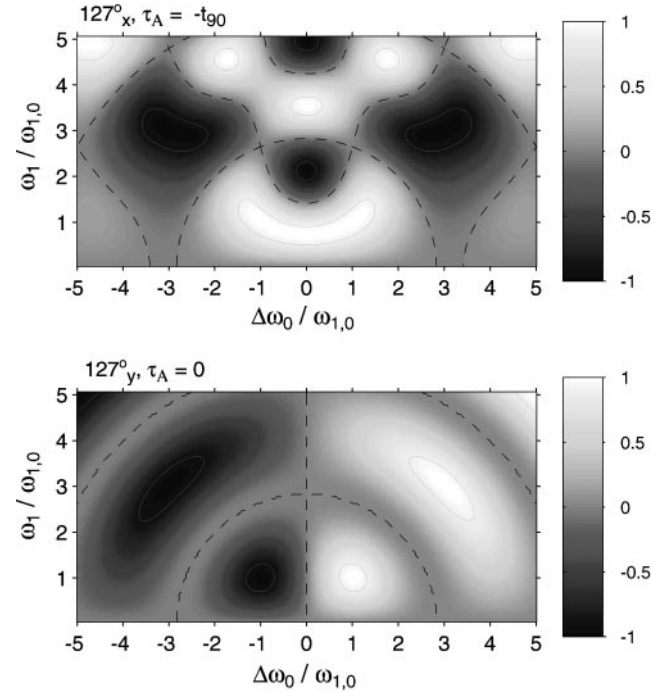

FIG. 9. Transverse y magnetization, m_y, following initial $\sqrt{2}90^\circ$ pulse. (Top) y magnetization following $\sqrt{2}90^\circ_0$ pulse and a period of free precession of duration $\tau_{\mathcal{A}} = -t_{90}$. (Bottom) y magnetization following $\sqrt{2}90^\circ_{90}$ pulse without any additional free precession period. The magnetization m_y is normalized with respect to M_0, the solid contour lines indicate $m_y = \pm 0.9$, and the dashed ones indicate $m_y = 0$. Note that in both cases, the magnetization near $\Delta\omega_0 = \pm(2k-1)\omega_{1,0}$; $\omega_1 = (2k-1)\omega_{1,0}$ is completely in the transverse plane and along the $\pm y$ axis.

and the spectrum of the asymptotic echo will be antisymmetric in frequency. Alternatively, a 127°_x pulse, followed by a period of free precession for duration $\tau_{\mathcal{A}} = -t_{90}$, rotates the initial $\hat{z}$ magnetization onto the $+\hat{y}$ axis for both $\Delta\omega_0 = \pm\omega_{1,0}$. This results in a symmetric spectrum of the asymptotic echo. The two off-resonance pulse sequences are therefore given by

$$127^\circ_0\text{–}(127^\circ_0\text{–}127^\circ_{180})^n \quad \text{with} \quad \tau_{\mathcal{A}} = -t_{90} \qquad [14]$$

$$127^\circ_{90}\text{–}(127^\circ_0\text{–}127^\circ_{180})^n \quad \text{with} \quad \tau_{\mathcal{A}} = 0. \qquad [15]$$

The experimental results shown in Fig. 5E and 5F confirm this analysis. For the symmetric distribution of Larmor frequencies in our sample, the symmetric sequence [14] results in a symmetric, in-phase echo signal and no out-of-phase signal. In contrast, the antisymmetric sequence [15] produces no in-phase signal and an antisymmetric echo signal in the out-of-phase channel.

3.4. Comparison of Different Broadband Pulses

The examples above illustrate the power of our new approach in designing pulse sequences for grossly inhomogeneous fields. It is apparent that many more sequences can be constructed with different properties. For instance, Fig. 7 shows that the refocusing pulse 90°_{45}–90°_{135}–90°_{45} can be easily modified to refocus magnetization near $(\Delta\omega_0/\omega_{1,0}, \omega_1/\omega_{1,0}) = (\pm[2k-1], [2k-1])$, by simply lengthening all the pulses by a factor of $\sqrt{2}$. Therefore, we see immediately that the sequence 127°_0–$(127^\circ_{45}$–127°_{135}–$127^\circ_{45})^n$ with $\tau_{\mathcal{A}} = 0$ has similar properties off-resonance at $\pm\omega_{1,0}$ as the antisymmetric sequence [15], but in addition will refocus some of the magnetization on resonance.

The results for all sequences shown in Fig. 5 confirm that the shapes of the echoes quickly approach an asymptotic limit after only a small number of echoes. In Fig. 10, we compare the asymptotic echoshapes and the corresponding spectra for the six sequences. The comparison of the first two spectra shows that choosing the correct value for $\tau_{\mathcal{A}}$ increases the bandwidth for the standard CPMG sequence significantly. Close to resonance, the response of the sequence 90°_0–$(90^\circ_{135}$–270°_{225}–$90^\circ_{135})^n$ with $\tau_{\mathcal{A}} = -2t_{90}/\pi$ is the flattest of all sequences studied. This is in agreement with previous work (*8, 16*) that focused on modest inhomogeneities.

For sequences *A*, *B*, *E*, and *F*, the axis $\hat{n}_{\mathcal{B}}$ of the refocusing cycle has only transverse components along the $\hat{y}$ axis. This is reflected in the measured spectra: the spectra are all absorption-like and appear only in the $\hat{y}$ channel. This is in contrast to the sequences with Levitt-type composite pulses (*C* and *D*) that have spectral contributions in both the in-phase and the out-of-phase channel. The magnitudes of the last two spectra (*E* and *F*) are very similar. Comparison of the two measured spectra confirms that by changing the excitation pulse, we can control whether the two spectral lobes are excited with the same or opposite sign.

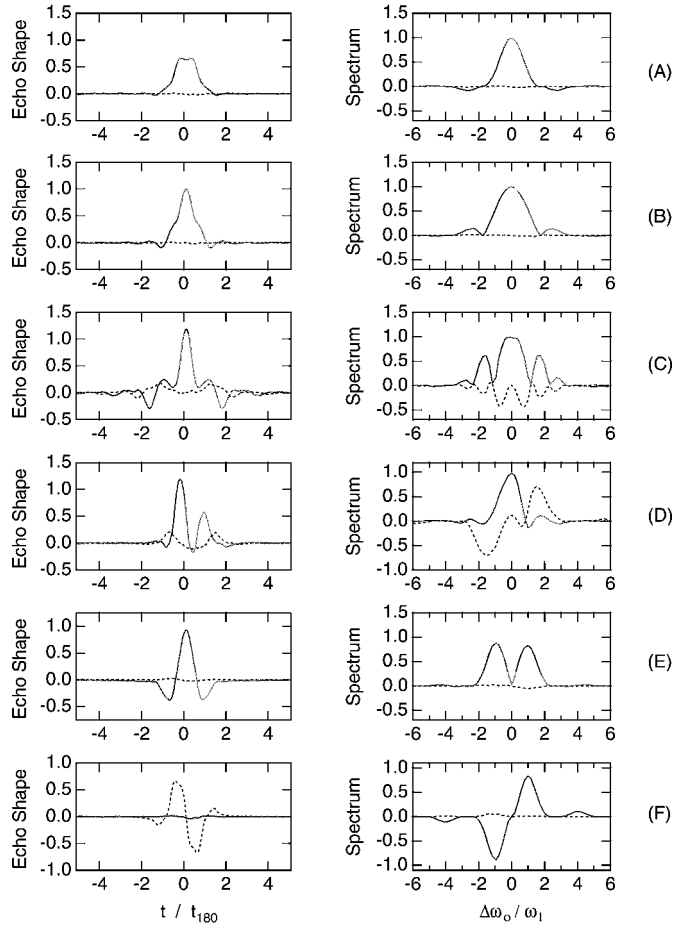

FIG. 10. Comparison of measured asymptotic echo shapes (left) and spectra (right) for six different CPMG-like sequences. The scale is kept the same for all sequences. In-phase signal is shown as a solid line, out-of-phase signal is dashed. (A) Standard CPMG sequence 90°_0–$(180^\circ_{90})^n$ with $\tau_{\mathcal{A}} = 0$. (B) Same as A, except $\tau_{\mathcal{A}} = -2t_{90}/\pi$. (C) CPMG with Levitt-type composite pulse with $\theta = 270^\circ$: 90°_0–$(90^\circ_{135}$–270°_{225}–$90^\circ_{135})^n$ with $\tau_{\mathcal{A}} = -2t_{90}/\pi$. (D) CPMG with Levitt-type composite pulse with $\theta = 90^\circ$: 90°_0–$(90^\circ_{45}$–90°_{135}–$90^\circ_{45})^n$ with $\tau_{\mathcal{A}} = 0$. (E) Symmetric off-resonance sequence 127°_0–$(127^\circ_0$–$127^\circ_{180})^n$ with $\tau_{\mathcal{A}} = -t_{90}$. (F) Antisymmetric off-resonance sequence 127°_{90}–$(127^\circ_0$–$127^\circ_{180})^n$ with $\tau_{\mathcal{A}} = 0$.

In Fig. 11, we demonstrate that all these sequences are suitable for measuring relaxation times. For each sequence, we used the corresponding asymptotic echo shape shown on the left of Fig. 10 as matched filter (*11*) to extract an echo amplitude for 400 echoes. For all sequences, the first few echo amplitudes show the characteristic transient behavior due to the second and third terms in Eq. [2] and already discussed in detail in (*6*) for the standard CPMG sequence. After the third echo, the echo amplitudes for all six sequences decay exponentially. Within experimental error, the time constants for the six sequences are identical and equal to the intrinsic relaxation time of the sample that was determined independently to be $T_1 = T_2 = 107$ ms. In these measurements, the echo spacing of 1 ms is short enough to make diffusion effects insignificant (*11*). For samples with $T_1 \neq T_2$, Eq. [4] predicts a slightly different decay rate

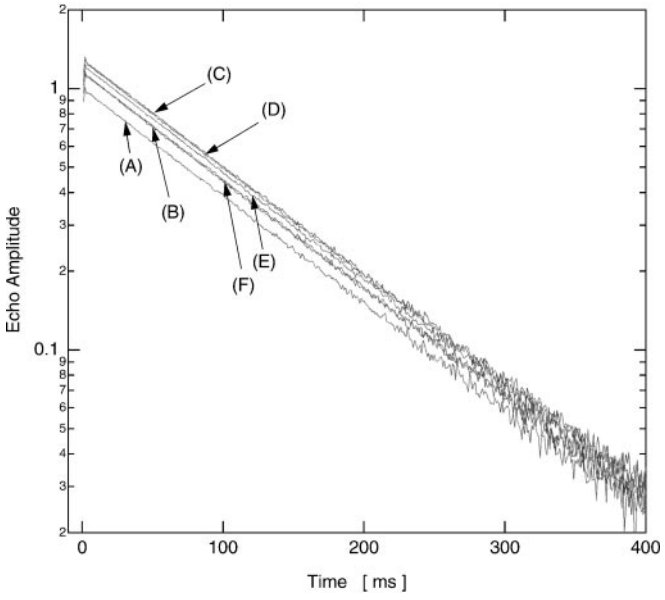

FIG. 11. Decay of echo amplitudes measured with the six different sequences. After the first few echoes, the amplitudes for every sequence decay exponentially with identical relaxation times. It equals the independently measured values $T_1 = T_2 = 107$ ms for this sample. The relative amplitudes are listed in Table 1. (A) 90°_0–$(180^\circ_{90})^n$ with $\tau_{\mathcal{A}} = 0$. (B) 90°_0–$(180^\circ_{90})^n$, $\tau_{\mathcal{A}} = -2t_{90}/\pi$. (C) 90°_0–$(90^\circ_{135}$–270°_{225}–$90^\circ_{135})^n$, $\tau_{\mathcal{A}} = -2t_{90}/\pi$. (D) 90°_0–$(90^\circ_{45}$–90°_{135}–$90^\circ_{45})^n$, $\tau_{\mathcal{A}} = 0$. (E) 127°_0–$(127^\circ_0$–$127^\circ_{180})^n$, $\tau_{\mathcal{A}} = -t_{90}$. (F) 127°_{90}–$(127^\circ_0$–$127^\circ_{180})^n$, $\tau_{\mathcal{A}} = 0$.

for the different sequences. This was not tested with the current measurements.

The echo amplitudes shown in Fig. 11 measured with different sequences decay with the same time constant, but have different overall amplitudes. In Table 1, we compare the relative echo amplitudes and the resulting increases in signal-to-noise ratio for the six sequences.

The relative signal-to-noise ratio is proportional to the square of the relative echo amplitude and is listed in the fourth column of Table 1. The measurements were made using a fixed RF field strength, or fixed peak power. Simply adjusting $\tau_{\mathcal{A}}$ to its optimum value for the standard CPMG sequence increases the echo amplitude by 15%, leading to a gain of over 1 dB in signal-to-noise ratio. Using the simple composite pulses in C and D, the signal-to-noise can be further improved by over 1 dB. If the limiting factor is not the peak power, but the average power P_{ave}, the advantage of these sequences disappears. In a constant gradient and fixed echo spacing, the signal-to-noise ratio for a given sequence scales like $S/N \propto P_{\text{ave}}$. The average power in turn is to a good approximation proportional to the duration of the refocusing pulse, which is listed in the third column of Table 1. Based on these scaling arguments, we calculate the expected relative signal-to-noise ratio of the different sequences using fixed average power and list them in the last column of Table 1. The results show that with constant average power, the standard CPMG sequence with the optimal value of $\tau_{\mathcal{A}}$, sequence B, is superior to the other sequences considered.

TABLE 1

Comparison of Relative Echo Amplitudes, Pulse Durations, and Signal-to-Noise-Ratios for Fixed Peak Power and for Fixed Average Power for the Six Sequences Listed in Fig. 5

			(S/N) (dB)	
Sequence	Rel. amp.	Pulse duration	Fixed P_{peak}	Fixed P_{ave}
A	1	t_{180}	0	0
B	1.15	t_{180}	+1.2	+1.2
C	1.30	$5/2\,t_{180}$	+2.3	−1.7
D	1.28	$3/2\,t_{180}$	+2.1	+0.4
E	1.23	$\sqrt{2}\,t_{180}$	+1.8	+0.3
F	1.16	$\sqrt{2}\,t_{180}$	+1.3	−0.2

4. CPMG SEQUENCES WITH NOVEL B_1 DEPENDENCIES

In the previous section, we have concentrated on pulse sequences that have interesting properties in the presence of strongly inhomogeneous B_0 fields. Here we show that using the same approach, we can also design novel pulse sequences that exhibit improved performance in the presence of strongly inhomogeneous B_1 fields.

To measure the B_1 dependence of a sequence experimentally, we kept our experimental setup, having a homogeneous RF field and a constant B_0 gradient across the sample, but we repeated the measurement with 25 different RF field strengths in the range of $0.92\omega_{1,0}$ to $3.13\omega_{1,0}$. The timing of the sequence was kept identical.

In Fig. 12 we show the measured $B_0 - B_1$ dependencies of the asymptotic echoes for three different sequences. In the top two panels, results are shown for the standard CPMG with two different values for $\tau_{\mathcal{A}}$. These results of the CPMG sequence show that in the vicinity of resonance, $\Delta\omega_0 \approx 0$, the echo amplitudes change sign when the RF strength is increased threefold. In the presence of sufficiently inhomogeneous RF fields, signals from different regions will therefore cancel each other and reduce the signal-to-noise ratio. Note that regions with different offset frequencies, $\Delta\omega_0$, do not pose the same problem. Such signals appear with different Larmor frequencies and even though they might interfere destructively at the nominal echo center, they will interfere constructively elsewhere without a reduction of overall signal-to-noise ratio.

Before we proceed with discussing new pulse sequences, we want to call attention to another feature apparent in the data shown in Figs. 12A and 12B: these results confirm that for the standard CPMG sequence, the optimal value of $\tau_{\mathcal{A}}$ depends on ω_1, as predicted by Eq. [11]. The delay for (B) of $\tau_{\mathcal{A}} = -2t_{90}/\pi$ was chosen to optimize the bandwidth for $\omega_1 = \omega_{1,0}$, as discussed before. The measurements show that at $3\omega_{1,0}$, this timing reduces the signal bandwidth compared to the timing $\tau_{\mathcal{A}} = 0$. This is expected based on Eq.[11], because $\tau_{\mathcal{A}} = 0$ is closer than $\tau_{\mathcal{A}} = -2t_{90}/\pi$ to the optimal value of $+2t_{90}/3\pi$ for this RF field strength.

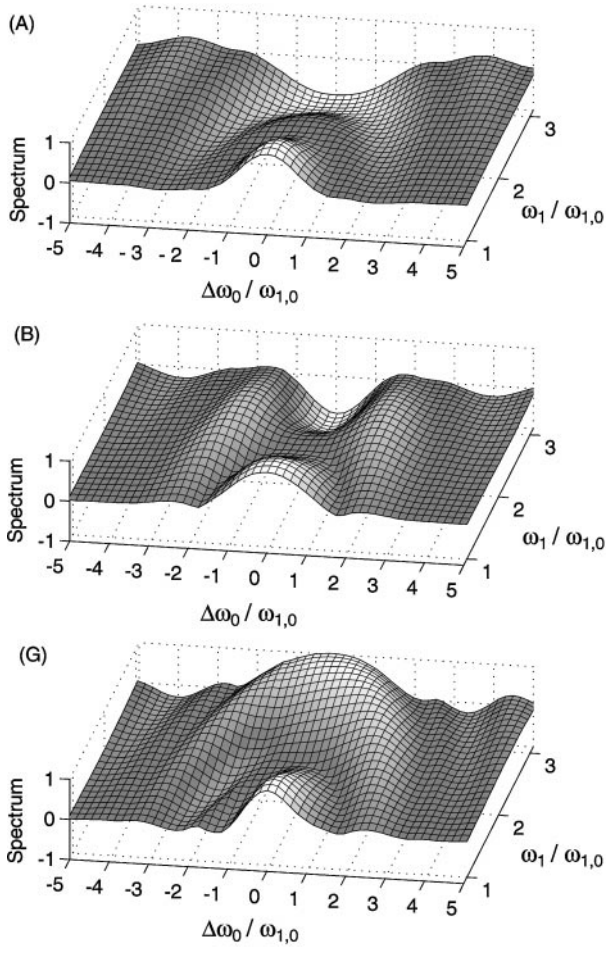

FIG. 12. Measured in-phase spectra of asymptotic echoes versus RF field strength, $\omega_1/\omega_{1,0}$, for three different sequences. (A) Standard CPMG sequence 90°_0–$(180^\circ_{90})^n$ with $\tau_{\mathcal{A}} = 0$. (B) Same as A, except $\tau_{\mathcal{A}} = -2t_{90}/\pi$. (G) Composite 90° pulse: $(45^\circ_{-45}$–$90^\circ_{45})$–$(180^\circ_{90})^n$ with $\tau_{\mathcal{A}} = 0$.

4.1. *Sequences without Signal Inversion at* $\omega_1 = 3\omega_{1,0}$

The change of sign in the standard CPMG signal at $3\omega_{1,0}$ is caused by the initial nominal 90° pulse. At $3\omega_{1,0}$, the initial pulse acts as a 270° pulse and rotates the magnetization onto the $-\hat{y}$ axis, while the direction of $\hat{n}_{\mathcal{B}}$ is still along the $\hat{y}$ direction. This combination leads to a negative signal. To avoid this, the standard 90° pulse must be replaced by a composite pulse that rotates the initial magnetization onto the positive $\hat{y}$ axis for all relevant RF field strengths. One solution is to use a half adiabatic fast passage with the RF ending on resonance along the $\hat{y}$ channel. This approach works for any value of ω_1 as long as the adiabatic condition is fulfilled. For a more limited range of ω_1 values, it is possible to use simple composite pulses instead.

The simplest composite 90° pulse that rotates magnetization from the $+\hat{z}$ direction onto the $+\hat{y}$ direction for both $\omega_{1,0}$ and $3\omega_{1,0}$ is the binary pulse 45°_{-45}–90°_{45}. Figure 13 shows the amplitude of the y component of the resulting magnetization following this composite 90° pulse as a function of offset frequency and RF field strength. On resonance, this pulse acts as a nominal 90°_x pulse for an RF field strength of both $\omega_{1,0}$ and $3\omega_{1,0}$. More complicated composite pulses can be designed that extend this behavior to higher odd multiples of $\omega_{1,0}$.

The bottom panel of Fig. 12 shows the measured ω_1 dependence of the asymptotic spectrum when the initial 90°_0 pulse of the CPMG sequence is replaced with the composite pulse 45°_{-45}–90°_{45}:

$$(45^\circ_{-45}\text{–}90^\circ_{45})\text{–}(180^\circ_{90})^n. \qquad [16]$$

These measurements confirm the theoretical analysis. With this simple modification of the sequence, the signal around resonance has now the same sign for RF strength in the range of 1 to $3\omega_{1,0}$. In the presence of inhomogeneous RF fields in this range, the asymptotic signals will all add coherently and not cancel each other. The out-of-phase spectrum of the asymptotic echoes still vanishes for all values of $\Delta\omega_0$ and ω_1 as with the standard CPMG sequence. In all three cases shown in Fig. 12, the spectra have no contributions when $\Delta\omega_0^2 + \omega_1^2 = (2\omega_{1,0})^2$. At these values, the refocusing pulses act as 360° pulses and do not refocus the magnetization.

4.2. *Selective Signal for* $\omega_1 = \omega_{1,0}$

In a different application, one might want to isolate signals that originate from regions with an RF field close to the nominal value, $\omega_{1,0}$. In grossly inhomogeneous RF fields, the standard CPMG sequence will generate significant signals at every odd multiple of the nominal field strength, $(2k+1)\omega_{1,0}$. This isolation can be achieved using a modified CPMG sequence with an initial pulse $\mathcal{A}$ designed such that it projects the $\hat{z}$ magnetization onto the axis $\hat{n}_{\mathcal{B}}$ at the nominal field strength, $\omega_{1,0}$, but perpendicular to it at all odd multiples of $\omega_{1,0}$. With the standard 180°_y refocusing pulse, this implies that the composite pulse should tip the $\hat{z}$ magnetization onto the $\hat{y}$ axis at $\omega_1 = \omega_{1,0}$ and onto the $\hat{x}$–$\hat{z}$ plane for $\omega_1 = (2k+1)\omega_{1,0}$, where $k = 1, 2, \ldots$.

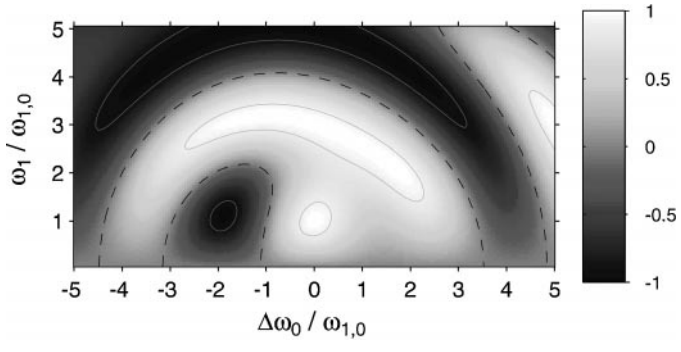

FIG. 13. Transverse y magnetization following 45°_{-45}–90°_{45} composite pulse applied to initial $\hat{z}$ magnetization. The displayed magnetization is normalized with respect to M_0, the solid contour lines indicate $m_y = \pm 0.9$, and the dashed ones indicate $m_y = 0$. On resonance, this pulse acts as a nominal 90°_x pulse at RF field strength of both $\omega_{1,0}$ and $3\omega_{1,0}$.

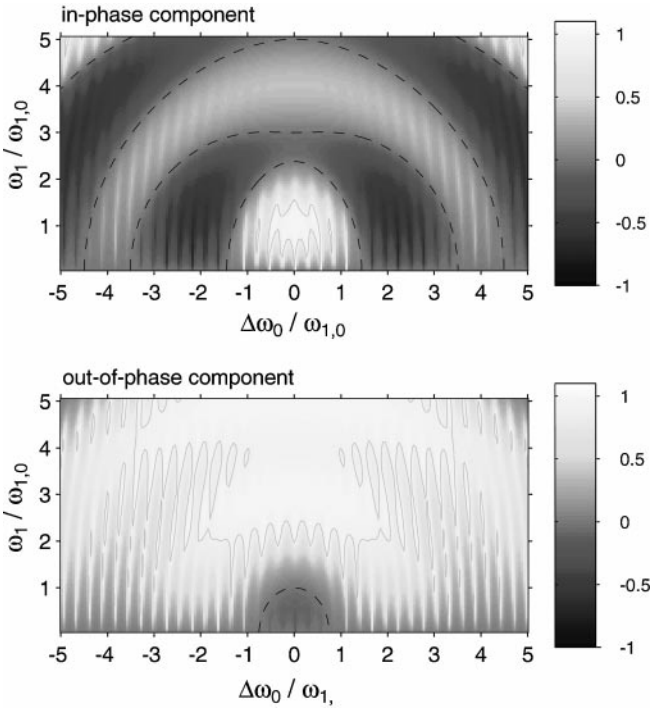

FIG. 14. Transverse components of axis characterizing refocusing cycle with composite pulse $90^\circ_{67.5}$–$45^\circ_{157.5}$–$90^\circ_{67.5}$. The solid contour lines indicate $n_{\mathcal{B},x,y} = 0.9$, the dashed lines $n_{\mathcal{B},x,y} = 0$. Note that near resonance, the axes $\hat{n}_{\mathcal{B}}$ for $\omega_1 = \omega_{1,0}$ and $\omega_1 = 3\omega_{1,0}$ are both in the transverse plane, but perpendicular to each other.

The binary composite pulse $45^\circ_{90-2\theta}$–$60^\circ_{90-\theta}$, where $\theta = 54.74^\circ$ is the magic angle, fulfills these conditions for the first three odd multiples, $k = 1, 2, 3$. Therefore, the modified CPMG sequence

$$(45^\circ_{-19.5}\text{–}60^\circ_{35.3})\text{–}(180^\circ_{90})^n \qquad [17]$$

has a maximum response around $\omega_1 = \omega_{1,0}$ but does not generate an asymptotic signal for $\omega_1 = 3, 5$, and $7\omega_{1,0}$.

4.3. B_1 Imaging

As was pointed out before, contributions from regions with different values of B_0 can be distinguished by Fourier transformation of the echo signal. However, contributions from regions with different RF field strengths cannot be separated in a similar way. Here we demonstrate a new CPMG sequence using composite pulses that can overcome this shortcoming to some degree. The main idea is to take advantage of the signal *phase*.

For the standard CPMG sequence, the phase of the spectrum of the asymptotic signal is always $\pm\hat{y}$, independent of the B_0 and B_1 distributions characterizing the sample. The out-of-phase spectrum only contains noise contributions. We can overcome this limitation and design sequences with composite pulses that encode information on RF field strength in the signal phase. For this purpose, we must find composite 180° pulses where the direction of the net axis $\hat{n}_{\mathcal{B}}$ depends on ω_1, coupled with excitation sequences $\mathcal{A}$ that are matched to these refocusing pulses, i.e., that maximize $\hat{n}_{\mathcal{B}} \cdot \mathcal{R}_{\mathcal{A}}\{\hat{z}\}$.

In Section 3.2, we showed that on resonance and for the nominal RF field strength, $\omega_1 = \omega_{1,0}$, pulses of the form $90^\circ_{90-\theta/2}$–$\theta_{180-\theta/2}$–$90^\circ_{90-\theta/2}$ act for all values of θ as 180°_y refocusing pulses. Among this class of pulses, the pulse with $\theta = 45^\circ$ is suitable for the purpose of B_1 imaging. The transverse components of the net axis $\hat{n}_{\mathcal{B}}$ for the composite refocusing pulse $90^\circ_{67.5}$–$45^\circ_{157.5}$–$90^\circ_{67.5}$ are shown in Fig. 14 as a function of frequency offset, $\Delta\omega_0$, and RF field strength, ω_1. It shows that at the nominal RF strength, $\omega_1 \approx \omega_{1,0}$, and in the vicinity of resonance, $\Delta\omega_0 \approx 0$, $\hat{n}_{\mathcal{B}}$ is pointing in the $\hat{y}$ direction and therefore this composite pulse refocuses the $\hat{y}$ component of the magnetization. In contrast, at $\omega_1 \approx 3\omega_{1,0}$, $\hat{n}_{\mathcal{B}}$ is pointing along the $\hat{x}$ direction and the asymptotic signal will have a different phase.

To take advantage of this refocusing pulse, we also must find an excitation pulse that rotates the initial $\hat{z}$ magnetization onto the $\hat{y}$ axis for $\omega_1 = \omega_{1,0}$ and onto the $\hat{x}$ axis for $\omega_1 = 3\omega_{1,0}$. The simplest such pulse is $22.5^\circ_{67.5}$–$90^\circ_{-22.5}$. In Fig. 15, the transverse

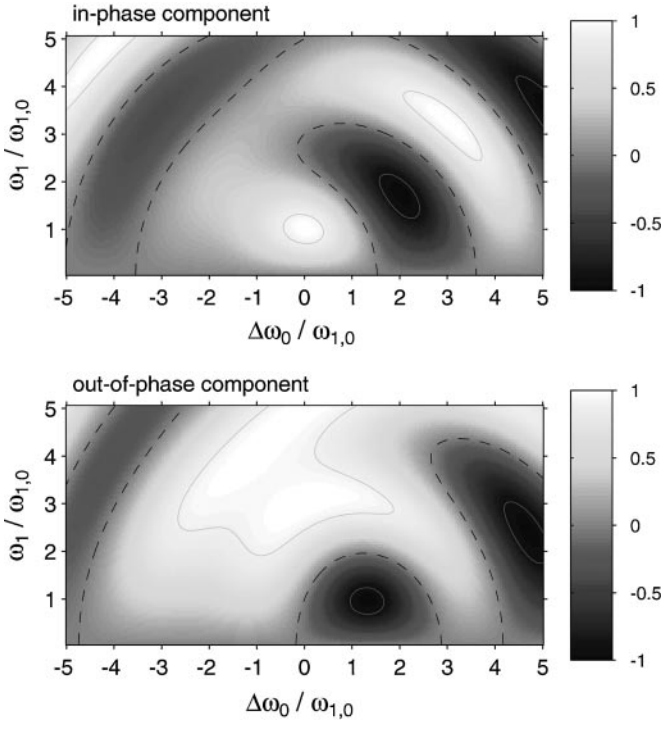

FIG. 15. Transverse magnetization following $22.5^\circ_{67.5}$–$90^\circ_{-22.5}$ composite pulse. Top panel shows in-phase magnetization, m_y, and bottom panel shows out-of-phase magnetization, $-m_x$. The magnetization is assumed to be initially in thermal equilibrium. The displayed magnetization is normalized with respect to M_0, the solid contour lines indicate $m_{x,y} = \pm 0.9$, and the dashed ones indicate $m_{x,y} = 0$. Note that around resonance, $\Delta\omega_0 = 0$, and for the nominal RF field strength, $\omega_1 = \omega_{1,0}$, the magnetization is pointing along the y direction, whereas for three times larger RF field strength, $\Delta\omega_0 = 0$ and $\omega_1 = 3\omega_{1,0}$, the magnetization is out-of-phase and points along the $-x$ direction.

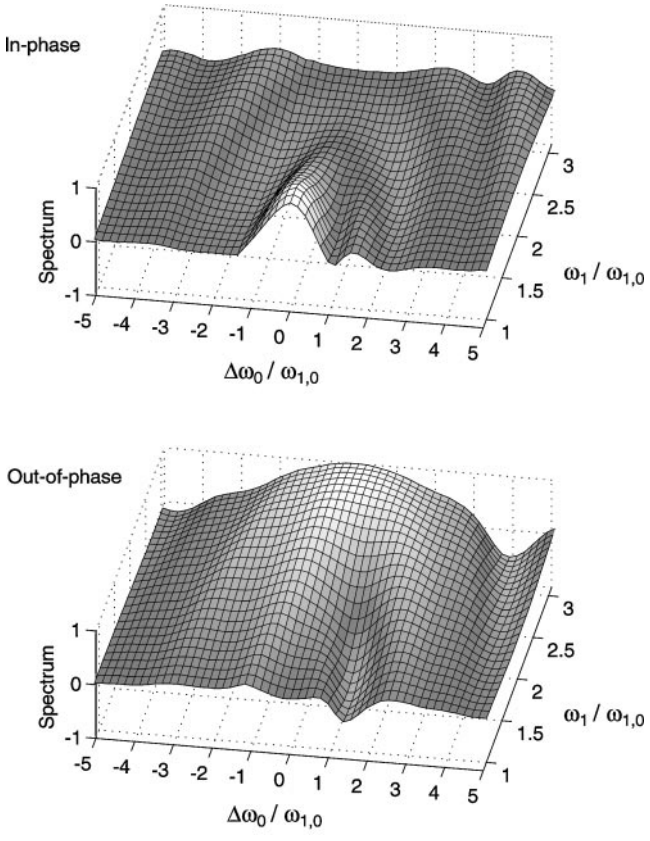

FIG. 16. B_1 imaging: Measured spectra of asymptotic echoes of composite pulse sequence $(22.5^\circ_{67.5}\text{–}90^\circ_{-22.5})\text{–}(90^\circ_{67.5}\text{–}45^\circ_{157.5}\text{–}90^\circ_{67.5})^n$ as a function of normalized RF field strength $\omega_1/\omega_{1,0}$. In-phase response, m_y, is shown on top, out-of-phase response, $-m_x$, at the bottom. For these measurements, $\tau_A = 0$.

magnetization following this pulse is shown. In the vicinity of resonance, this pulse indeed fulfills our requirement.

Combining the two elements, we can construct an example of a "B_1 imaging" CPMG sequence:

$$(22.5^\circ_{67.5}\text{–}90^\circ_{-22.5})\text{–}(90^\circ_{67.5}\text{–}45^\circ_{157.5}\text{–}90^\circ_{67.5})^n. \qquad [18]$$

Note that in this sequence, the phases of the individual pulses differ only by multiples of 90°.

We have tested this sequence experimentally. The results for the spectrum of the asymptotic echoes as a function of RF field strength are shown in Fig. 16. Not too far from resonance $-\omega_{1,0} < \Delta\omega_0 < \omega_{1,0}$ the signal for the nominal RF field strength, $\omega_1 \simeq \omega_{1,0}$, peaks in the in-phase channel and the contributions to the out-of-phase channel are small. At $3\omega_{1,0}$, the experimental results show that the situation is reversed. There is little signal in the in-phase channel, but maximal signal in the out-of-phase channel. This implies that we can clearly distinguish contributions from regions with RF field strength of $\omega_{1,0}$ and $3\omega_{1,0}$, i.e., a coarse way of B_1 imaging.

4.4. Comparison of On-resonance Behavior

We have demonstrated that using composite pulses, it is possible to design CPMG-like sequences that still have the inherent error compensation of the standard CPMG sequence and generate large asymptotic signals, but have modified B_1 dependencies. In Fig. 17, we summarize these modifications by comparing the measured responses close to resonance for three different sequences. The three sequences refocus all the magnetization along the $\hat{y}$ direction when the RF field strength equals the nominal RF field strength, $\omega_{1,0}$. With the standard CPMG, the signal vanishes when ω_1 reaches $2\omega_{1,0}$ and fully inverts at $3\omega_{1,0}$.

With the modified sequence $(45^\circ_{-45}\text{–}90^\circ_{45})\text{–}(180^\circ_{90})^n$, the sign of the signal does not change as the RF field strength is increased

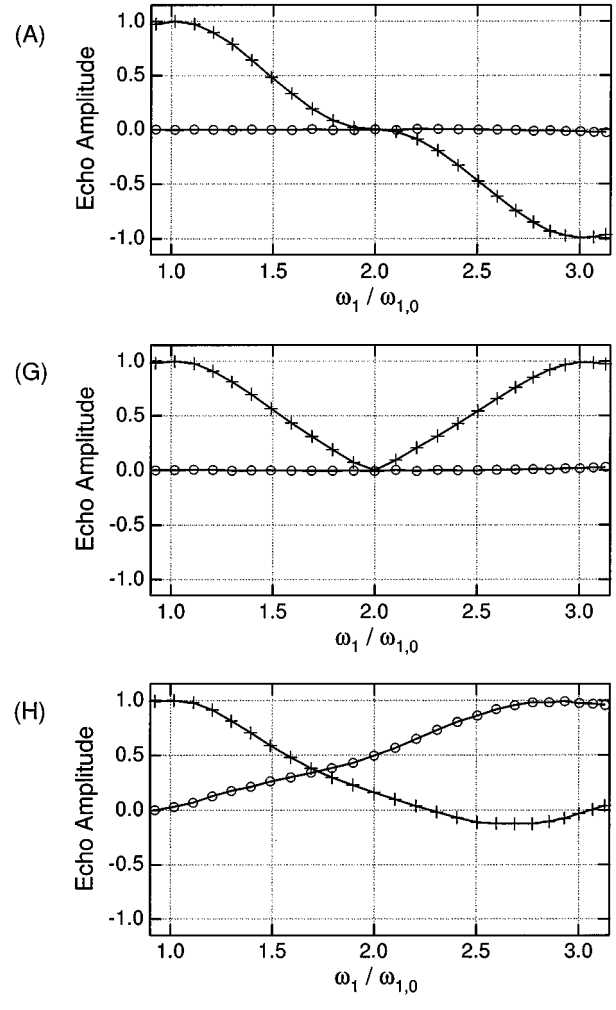

FIG. 17. On resonance asymptotic echo amplitudes versus normalized RF field strength, $\omega_1/\omega_{1,0}$ for three different sequences. In-phase amplitudes, m_y, are shown as crosses, out-of-phase amplitudes, $-m_x$, as circles. (A) Standard CPMG sequence $90^\circ_0\text{–}(180^\circ_{90})^n$. (G) Composite 90° pulse: $(45^\circ_{-45}\text{–}90^\circ_{45})\text{–}(180^\circ_{90})^n$. (H) Composite 90° and 180° pulses: $(22.5^\circ_{67.5}\text{–}90^\circ_{-22.5})\text{–}(90^\circ_{67.5}\text{–}45^\circ_{157.5}\text{–}90^\circ_{67.5})^n$. For sequence (H), the phase of the asymptotic echo is directly related to the RF field strength.

threefold. The magnitude of the signal at $3\omega_{1,0}$ is identical to the signal at $\omega_{1,0}$, indicating that the full magnetization is refocused. At intermediate RF field strengths around $2\omega_{1,0}$, the signal magnitude generally exceeds the magnitude of the signal acquired with the standard CPMG sequence. For both sequences, the out-of-phase signal vanishes for all values of RF strength.

With the third sequence, $(22.5^\circ_{67.5}–90^\circ_{-22.5})–(90^\circ_{67.5}–45^\circ_{157.5}–90^\circ_{67.5})^n$, the signal magnitude does not depend as strongly on RF field strength as with the previous two sequences and it does not vanish anymore at $2\omega_{1,0}$. The bottom panel in Fig. 17 shows clearly that the phase of the signal is changing continuously by $\pi/2$ as the RF field strength is changed from $\omega_{1,0}$ to $3\omega_{1,0}$. Therefore, the phase of the signal can be used directly to infer the strength of the RF field.

Analogous to the sequences discussed in Section 3, these sequences are also useful for measuring relaxation times. In inhomogeneous fields, the signal amplitudes show the transient behavior for the first few echoes and then decay with the relaxation times characteristic of the sample.

5. CONCLUSIONS

We have developed a new approach for designing modified CPMG-like sequences with composite pulses that maintain the error-correcting properties of the original CPMG sequence. We have demonstrated new sequences that exhibit improved signal-to-noise ratio in grossly inhomogeneous fields and that are suitable for relaxation time measurements. Using this approach, it is also possible to shape the excitation bandwidth. For example, one of the new sequences produces echoes with a bimodal spectrum in inhomogeneous fields. Depending on the details of the initial pulse, the spectrum can be excited with either an even or an odd symmetry. We have also demonstrated sequences with novel B_1 dependencies that improve the performance in very inhomogeneous B_1 fields or that allow coarse B_1 imaging.

Our new approach is based on Eq. [3]. This expression describes the asymptotic magnetization that forms coherently from echo to echo and decays with the relaxation time characteristic of the sample. The other components of the magnetization dephase rapidly in inhomogeneous fields and only contribute to the initial amplitude transient observed for the first few echoes. We have taken advantage of the simple geometrical interpretation of Eq. [3].

By concentrating on the asymptotic magnetization, the complicated full expression for an echo following a large number of pulses gets reduced to a simple expression that only involves the initial excitation pulse and the properties of a single refocusing cycle. This makes it possible to gain new insights into the relevant spin dynamics and find new sequences that are optimized for different specific properties. We have shown that it is essential to match the excitation pulse with the refocusing cycle such that the initial transverse magnetization lies along the axis $\hat{n}_{\mathcal{B}}$ characterizing the overall rotation by the refocusing cycle. This can be achieved by choosing the overall phase shift between the initial pulse and refocusing pulses appropriately on resonance. Dispersion can be compensated to first order by proper choice of the time interval $\tau_{\mathcal{A}}$ defined in Fig. 1.

In this paper, we have concentrated on simple composite pulses. However, our approach is general and can be used with more complicated composite pulses or with elements involving frequency sweeps or other modulations. It is also straightforward to refine the optimization of the composite pulses discussed here by using a numerical search routines that take into account the specific experimental parameter space of interest, additional constraints, and the desired optimization function.

ACKNOWLEDGMENTS

I thank D. Freed and P. Sen for useful discussions.

REFERENCES

1. H. Y. Carr and E. M. Purcell, Effects of diffusion on free precession in nuclear magnetic resonance experiments, *Phys. Rev.* **94,** 630–638 (1954).
2. S. Meiboom and D. Gill, Modified spin-echo method for measuring nuclear relaxation times, *Rev. Sci. Instrum.* **29,** 688–691 (1958).
3. P. J. McDonald, Stray field magnetic resonance imaging, *Prog. Nucl. Magn. Reson. Spectrosc.* **30,** 69–99 (1997).
4. R. L. Kleinberg, Well logging, *in* "Encyclopedia of Nuclear Magnetic Resonance," Vol. 8, pp. 4960–4969. Wiley, Chichester (1996).
5. G. Eidmann, R. Savelsberg, P. Blümler, and B. Blümich, The NMR MOUSE, a mobile universal surface explorer, *J. Magn. Reson. A* **122,** 104–109 (1996).
6. M. D. Hürlimann and D. D. Griffin, Spin dynamics of Carr–Purcell–Meiboom–Gill-like sequences in grossly inhomogeneous B_0 and B_1 fields and application to NMR well logging, *J. Magn. Reson.* **143,** 120–135 (2000).
7. G. Goelman and M. G. Prammer, The CPMG pulse sequence in strong magnetic field gradients with applications to oil-well logging, *J. Magn. Reson. A* **113,** 11–18 (1995).
8. J. Simbrunner and R. Stollberger, Analysis of Carr–Purcell sequences with nonideal pulses, *J. Magn. Reson. B* **109,** 301–309 (1995).
9. A. Ross, M. Czisch, and G. C. King, Systematic errors asssociated with the CPMG pulse sequence and their effect on motional analysis of biomolecules, *J. Magn. Reson.* **124,** 355–365 (1997).
10. F. Bălibanu, K. Hailu, R. Eymael, D. E. Demco, and B. Blümich, Nuclear magnetic resonance in inhomogeneous magnetic fields, *J. Magn. Reson.* **145,** 246–258 (2000).
11. M. D. Hürlimann, Diffusion and relaxation effects in general stray field NMR experiments, *J. Magn. Reson.* **148,** 367–378 (2001).
12. M. H. Levitt and R. Freeman, NMR population inversion using a composite pulse, *J. Magn. Reson.* **33,** 473–476 (1979).
13. M. H. Levitt and R. Freeman, Compensation for pulse imperfections in NMR spin-echo experiments, *J. Magn. Reson.* **43,** 65–80 (1981).
14. M. H. Levitt and R. R. Ernst, Composite pulses constructed by a recursive expansion procedure, *J. Magn. Reson.* **55,** 247–254 (1983).
15. A. J. Shaka and R. Freeman, Composite pulses with dual compensation, *J. Magn. Reson.* **55,** 487–493 (1983).
16. R. Tycko, Broadband population inversion, *Phys. Rev. Lett.* **51,** 775–777 (1983).

17. R. Tycko, H. M. Cho, E. Schneider, and A. Pines, Composite pulses without phase distortion, *J. Magn. Reson.* **61,** 90–101 (1985).
18. R. Tycko, A. Pines, and J. Guckenheimer, Fixed point theory of iterative excitation schemes in NMR, *J. Chem. Phys.* **83,** 2775–2802 (1985).
19. A. J. Shaka and A. Pines, Symmetric phase-alternating composite pulses, *J. Magn. Reson.* **71,** 495–503 (1987).
20. H. M. Cho and A. Pines, Iterative maps for broadband excitation of transverse coherence in two level systems, *J. Chem. Phys.* **86,** 6591–6601 (1987).
21. S. Wimperis, Iterative schemes for phase-distortionless composite 180° pulses, *J. Magn. Reson.* **93,** 199–206 (1991).
22. M. H. Levitt, Composite pulses, *Prog. Nucl. Magn. Reson. Spectrosc.* **18,** 61–122 (1986).
23. A. J. Shaka, S. P. Rucker, and A. Pines, Iterative Carr-Purcell trains, *J. Magn. Reson.* **77,** 606–611 (1988).
24. M. H. Levitt, R. Freeman, and T. Frenkiel, Broadband decoupling in high-resolution nuclear magnetic resonance spectroscopy, *Adv. Magn. Reson.* **11,** 47–110 (1983).
25. T. Gullion, D. B. Baker, and M. S. Conradi, New, compensated Carr–Purcell sequences, *J. Magn. Reson.* **89,** 479–484 (1990).
26. T. Gullion, The effect of amplitude imbalance on compensated Carr–Purcell sequences *J. Magn. Reson. A* **101,** 320–323 (1993).
27. A. Abragam, "Principles of Nuclear Magnetism." Clarendon Press, Oxford, (1978).
28. J. Baum, R. Tycko, and A. Pines, Broadband population inversion by phase modulated pulses, *J. Chem. Phys.* **79,** 4643–4644 (1983).
29. K. Uğurbil, M. Garwood, and M. R. Bendall, Amplitude- and frequency-modulated pulses to achieve 90° plane rotations with inhomogeneous B_1 fields, *J. Magn. Reson.* **72,** 177–185 (1987).
30. K. Uğurbil, M. Garwood, A. R. Rath, and M. R. Bendall, Amplitude- and frequency/phase-modulated refocusing pulses that induce plane rotations even in the presence of inhomogeneous B_1 fields, *J. Magn. Reson.* **78,** 472–497 (1988).
31. M. Garwood and Y. Ke, Symmetric pulses to induce arbitrary flip angles with compensation for RF inhomogeneity and resonance offsets, *J. Magn. Reson.* **94,** 511–525 (1991).
32. S. Conolly, D. Nishimura, and A. Macovski, A selective adiabatic spin-echo pulse, *J. Magn. Reson.* **83,** 324–334 (1989).
33. T. Hwang, P. C. M. van Zijl, and M. Garwood, Broadband adiabatic refocusing without phase distortion, *J. Magn. Reson.* **124,** 250–254 (1997).
34. M. Zweckstetter and T. A. Holak, An adiabatic multiple spin-echo pulse sequence: Removal of systematic errors due to pulse imperfections and off-resonance effects, *J. Magn. Reson.* **133,** 134–147 (1998).
35. C. Counsell, M. H. Levitt, and R. R. Ernst, Analytical theory of composite pulses, *J. Magn. Reson.* **63,** 133–141 (1985).
36. D. J. Lurie, Numerical design of composite radiofrequency pulses, *J. Magn. Reson.* **70,** 11–20 (1986).
37. C. S. Poon and R. M. Henkelman, 180° refocusing pulses which are insensitive to static and radiofrequency field inhomogeneity, *J. Magn. Reson.* **99,** 45–55 (1992).
38. C. S. Poon and R. M. Henkelman, Robust refocusing pulses of limited power, *J. Magn. Reson. A* **116,** 161–180 (1995).
39. N. S. Bai, M. Ramakrishna, and R. Ramachandran, Design of phase-distortionless broadband composite-pulse sequences via simulated annealing, *J. Magn. Reson. A* **102,** 235–240 (1993).
40. M. D. Hürlimann, Optimization of timing in the Carr–Purcell–Meiboom–Gill sequence, *Magn. Reson. Imaging*, in press.